

**$W^0$  effects in electron-positron collisions on  $1^-$  resonances**

Robert Budny\*

*Joseph Henry Laboratories, Princeton University, Princeton, New Jersey 08540*

(Received 30 January 1979)

Cross sections are given for  $e^-e^+$  collisions on  $1^-$  resonances producing pairs of spin-1/2 particles in the tree approximation. Effects of neutral currents and beam polarization are included. Possibilities for measuring  $W^0$  effects in collisions producing  $\mu^-\mu^+$ ,  $\tau^-\tau^+$ , and  $e^-e^+$  at the  $T$  and higher-mass resonances are discussed.

I. INTRODUCTION

We are learning much about weak neutral currents from neutrino scattering, from polarized-electron scattering, and from parity-violating effects in atomic and nuclear transitions. We can expect to learn more from  $e^-e^+$  collisions at high energies. For instance, by approaching the pole in the  $W^0$  propagator we can learn the  $W^0$  mass. Perhaps we will find surprises such as additional  $W^0$ 's. Also, we may be able to measure  $W^0$  couplings of unstable particles such as resonances and heavy leptons.

Many papers have studied the prospects of measuring weak effects in  $e^-e^+$  collisions.<sup>1-4</sup> A problem is that the center-of-momentum energy  $W = \sqrt{s}$  should be large to enhance the signal-to-noise ratio, but at large  $W$  the event rates of many specific channels are small. It may be possible to enhance the signal (along with the noise) using resonances. If resonances such as the  $T$  family<sup>5-7</sup> couple appreciably to  $e^-e^+$ , they could provide such enhancements.

These enhancements are reduced by spreading caused by radiative corrections and the distribution of energies in the beams. For example, consider a narrow spin-1 resonance of mass  $M_0$  in  $e^-e^+ \rightarrow f$ . The Breit-Wigner formula for the cross section is

$$\sigma_{BW}(s) = \frac{12\pi M_0^2}{s} \frac{\Gamma_e \Gamma_f}{(s - M_0^2)^2 + M_0^2 \Gamma^2} \quad (1.1)$$

If  $W$  is larger than  $M_0$ , the electron or positron can radiate the excess energy and collide on resonance, so the cross section with beam-bremsstrahlung corrections has a ramp as sketched in Fig. 1.

Since the energy in the beams is spread, the radiatively corrected cross section must be folded with the beam distributions, giving a softer observed cross section. In the case where the distribution of  $W$  is a Gaussian of width  $\sigma_w$ , and the

resonance is very narrow ( $\Gamma \ll \sigma_w$ ), the cross section at  $M_0^2$  is reduced to<sup>8</sup>

$$\sigma(M_0^2)_{res} = \frac{K}{\sigma_w \sqrt{2\pi}} \frac{\pi \Gamma}{2} \sigma_{BW}(M_0^2) \quad (1.2)$$

Here,

$$K = \left( \frac{2\sqrt{2}\sigma_w}{M_0} \right)^\epsilon (1 + 0.79\epsilon)$$

is the reduction caused by radiation with

$$\epsilon = \frac{2\alpha}{\pi} \left[ \ln \left( \frac{M_0^2}{M_e^2} \right) - 1 \right]$$

A typical value for  $\sigma_w$  is 4.3 MeV at  $W = 9.5$  GeV. (The full width at half maximum is  $2.35 \sigma_w$ .) The corresponding values of  $K$  and  $\epsilon$  are 0.60 and 0.087, respectively. They do not vary much over the range of  $\sigma_w$  and  $W$  anticipated for the PETRA, CESR, and PEP facilities.

This implies that the enhancements of  $e^-e^+ \rightarrow \mu^-\mu^+$  and  $e^-e^+ \rightarrow$  hadrons caused by the resonance, relative to the nonresonating backgrounds (to lowest order), are

$$\mathcal{G}_\mu^0 = \frac{\sigma_\mu(M_0^2)_{res}}{4\pi\alpha^2/3M_0^2} = \frac{9\pi K \Gamma_e \Gamma_\mu}{2\sqrt{2}\pi\alpha^2\sigma_w\Gamma} \approx \frac{3.4\Gamma_e^2}{\alpha^2\sigma_w\Gamma}$$

and

$$\mathcal{G}_h^0 = \frac{\sigma_h(M_0^2)_{res}}{R_h 4\pi\alpha^2/3M_0^2} = \mathcal{G}_\mu^0 \frac{\Gamma_h}{\Gamma_\mu R_h} \quad (1.3)$$

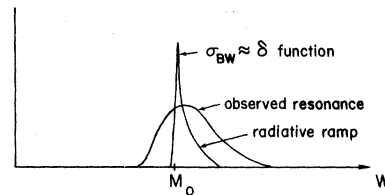


FIG. 1. Corrections giving the observed resonance part of the cross section.

with  $R_h \approx 5$  being the background ratio of hadrons to  $\mu^- \mu^+$ . The value of  $\mathcal{E}_\mu^0$  can be estimated using DASP data.<sup>7</sup> If  $\Gamma_e = 1.5$  keV and  $\Gamma = 60$  keV, then  $\mathcal{E}_\mu^0 = 0.56$ . This enhancement is discouragingly small, but perhaps enough events will be collected to measure weak effects.

Besides using resonances for enhancement, it may be possible to measure their couplings to the  $W^0$ . The amplitude for a resonance to decay includes the terms in Fig. 2. The relative magnitude of the photon- $W^0$  interference in a cross section is given by the ratio of amplitudes shown in Fig. 3, i.e.,

$$\frac{f_W G_{V,A} / M_W \omega^2}{f_Q e / M_T^2} \approx \frac{f_W}{f_Q} \left( \frac{M_T}{M_W} \right)^2. \quad (1.4)$$

This is expected to be of the order of 0.01 for  $M_T = 9.46$  GeV. The ratio of  $W^0$  to  $\gamma$  coupling of resonances  $f_W/f_Q$  would be an interesting quantity to know. The imprecisely known bound-state wave function of the resonances should occur equally in  $f_W$  and  $f_Q$ , and thus cancel, leaving the ratio of quark couplings. This ratio will be difficult to measure for reasons discussed below.

This paper gives the cross section for  $e^- e^+$  annihilation in the tree approximation. The amplitudes used are those in Fig. 4 with an arbitrary number of  $1^-$  resonances and arbitrary beam polarizations. The case  $e^- e^+ \rightarrow \mu^- \mu^+$  on a narrow  $1^-$  resonance is discussed in Sec. II. Narrow resonances appear to be nuisances for measuring  $W^0$  effects in this reaction. The prospects of measuring  $W^0$  effects in  $e^- e^+ \rightarrow \tau^- \tau^+$  by analyzing the  $\mu$  or  $e$  from  $\tau$  decays are discussed in Sec. III. It may be feasible to measure the ratio of couplings to resonances using this reaction. Also, the cross section for the Bhabha-type process including the  $t$ -channel analogs of the amplitudes in Fig. 4 is given. The case  $e^- e^+ \rightarrow e^- e^+$  is discussed in Sec. IV.

## II. $e^- e^+ \rightarrow \mu^- \mu^+$

This reaction is very clean in that backgrounds are relatively small. Also, the analysis is fairly straightforward. It can teach us properties of resonances such as their  $J^{PC}$  through photon-resonance interference.

To see what can be learned about  $W^0$  couplings, consider the case of unpolarized or transversely polarized beams of moderate energy. The cross

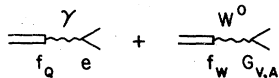


FIG. 2. Tree amplitudes for resonance decays.

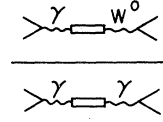


FIG. 3. Relative magnitude for photon- $W^0$  interference terms.

section from Appendix A is

$$\frac{d\sigma}{d\Omega} = \frac{\alpha^2}{4s} \left[ (1 + \cos^2\theta + \phi^- \phi^+ \sin^2\theta \cos 2\phi) \times (\mathcal{E}_\mu + 1)(1 + 2g_V^2 R) + 2 \cos\theta(2g_A^2 R) + \phi^- \phi^+ \sin^2\theta \sin 2\phi \mathcal{E}_\mu \frac{\alpha\Gamma}{3\Gamma_e} 2g_A(\rho - g_V)R \right]. \quad (2.1)$$

The terms containing  $R \equiv s[e^2(s - M_W^2)]^{-1}$  come from photon- $W^0$  interferences. (Terms containing  $R^2$  were dropped here for being small at moderate energies.) The couplings  $g_V$  and  $g_A$  are of the  $e$  and  $\mu$  to the  $W^0$ , and  $\rho$  is the charge of the electron times the ratio of the weak and electromagnetic couplings of the resonance. Their expressions in the Weinberg-Salam model are in Appendix A and are plotted in Fig. 5.

The effect of the resonance is the  $s$ -dependent  $\mathcal{E}_\mu$ . When the total width of the resonance is small, this enhancement has a width approximately  $\sigma_W$  and is peaked near  $s = M_0^2$ . The contribution to  $\mathcal{E}_\mu$  from beam corrections  $\mathcal{E}_\mu^0$  has the peak value given in Eq. (1.3). The weak corrections to  $\mathcal{E}_\mu^0$  are

$$\mathcal{E}_\mu / \mathcal{E}_\mu^0 \approx 1 + \delta = 1 + 2(2\rho - g_V)g_V R. \quad (2.2)$$

The magnitudes of  $\delta$  for  $t$  and  $b$  quarks in the Weinberg-Salam model are in Fig. 6. They are less than about 0.01 in this model with  $\sin^2\theta_W$  near 0.25. Measurements of  $\mathcal{E}_\mu$  will not reveal  $\delta$  due to various reasons—including the problem of not being able to know  $\mathcal{E}_\mu^0$  sufficiently accurately.

The  $\cos\theta$  term does not get a contribution from the resonance (to order  $R$ ) since it requires an axial-vector coupling to both the  $e$  and  $\mu$ ; but  $1^-$  resonances have only vector coupling to the  $W^0$ . This term could, in principle, be measured as a forward-backward asymmetry,

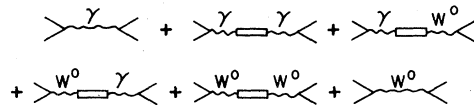


FIG. 4. Tree amplitudes for  $e^- e^+ \rightarrow F^- F^+$ .

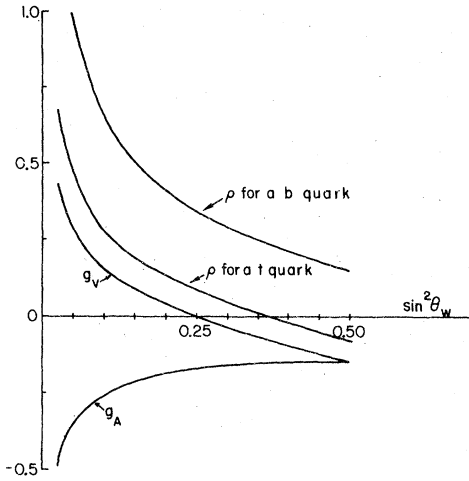


FIG. 5. Weak coupling constants versus  $\sin^2\theta_w$  in the Weinberg-Salam model with  $t$  and  $b$  quarks.

$$A_{FB} = \frac{N_F - N_B}{N_F + N_B} = \frac{\int_0^1 - \int_{-1}^0 d \cos\theta \frac{d\sigma}{d \cos\theta}}{\int_0^1 + \int_{-1}^0 d \cos\theta \frac{d\sigma}{d \cos\theta}} = \frac{3g_A^2 R}{2(\mathcal{E}_\mu + 1)}. \quad (2.3)$$

In the Weinberg-Salam model, the value of  $3g_A^2 R/2$  at  $W=9.46$  GeV is  $-0.006$ . This asymmetry could be measured with an integrated luminosity of  $1.1 \times 10^5 (1 + \mathcal{E}_\mu)/\text{nb}$ . Obviously, it would be quicker to measure off resonance where  $\mathcal{E}_\mu = 0$ .

Even if these weak corrections were not as small as the Weinberg-Salam model suggests, the measurements discussed above may give ambiguous information about weak couplings. This is because all but the  $\sin 2\phi$  term in  $d\sigma/d\Omega$  are even under parity ( $P$ ) and charge conjugation ( $C$ ), so higher-order electromagnetic effects can contribute, and mask out the  $W^0$  effects. They have been estimated to be of order 10% (off resonance).<sup>9</sup>

$$A_{\text{long}} = \frac{N(\phi_-^L, +\phi_+^L) - N(-\phi_-^L, -\phi_+^L)}{N(\phi_-^L, +\phi_+^L) + N(-\phi_-^L, -\phi_+^L)} = \left[ \frac{(\phi_-^L + \phi_+^L)(1 + \cos\theta)^2}{(1 + \phi_-^L \phi_+^L)(1 + \cos^2\theta) + \phi_-^L \phi_+^L \sin^2\theta \cos 2\phi} \right] \frac{2(\mathcal{E}_\mu \rho + g_V) g_A R}{\mathcal{E}_\mu + 1}. \quad (2.5)$$

The values of  $d_r \equiv 2g_A \rho R$  and  $d_b \equiv 2g_A g_V R$  from the Weinberg-Salam model are in Fig. 6.

Measuring  $A_{\text{long}}$  offers several features. It would test  $\mu$ - $e$  universality since the  $1 + \cos^2\theta$  and the  $2 \cos\theta$  parts in the numerator come from axial-vector coupling to the  $e$  and  $\mu$ , respectively. Also, in principle, a very precise measurement of  $A_{\text{long}}$  with one of the previously discussed measurements could yield  $\rho$ . Unfortunately it will be

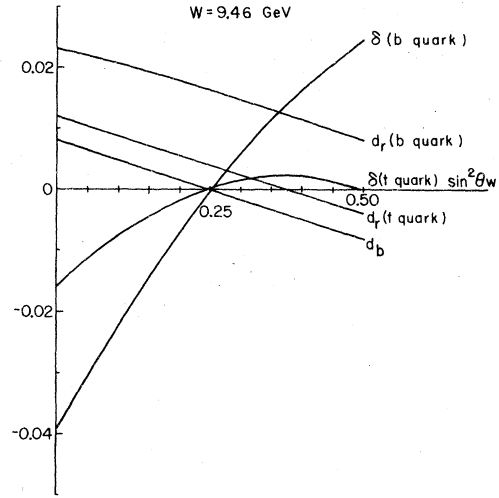


FIG. 6.  $W^0$  corrections to the asymmetry and enhancement from the Weinberg-Salam model at  $W=9.46$  GeV.

More precise calculations would be needed to separate  $W^0$  effects from the above measurements.

Terms odd under  $P$  or  $C$  would be less ambiguous signals of weak effects. The  $P$ - and  $C$ -odd  $\sin 2\phi$  term has an interesting coupling,  $2g_A(\rho - g_V)R$  which, in the Weinberg-Salam model, is 0.016 for a  $b$  quark at  $W=9.46$  GeV. Unfortunately, the factor

$$\mathcal{E}_\mu \frac{\alpha \Gamma}{3\Gamma_e} \approx 1.1 \frac{\Gamma_e}{\alpha \sigma_W} \quad (2.4)$$

is expected to be 0.05 for a  $b$  quark. Thus the  $\sin 2\phi$  term is too small to be measured at the  $\Upsilon(9.46)$ .

There are two other measurements of  $P$ -odd terms which are remotely feasible. One requires longitudinally polarized beams. If these can be constructed (presumably by rotating transversely polarized beams) then the asymmetry, when both are reversed, is

hard to measure  $A_{\text{long}}$  (except possibly at very large  $W$ ) since even if longitudinal polarization is feasible, it is expected to be small.

The other remotely feasible  $P$ -odd measurement is of a final helicity. To do this, one of the  $\mu^+$  would have to be stopped in order to watch the direction of its decay. This is very difficult for high-energy muons, and may be impossible due to depolarization as the muon is decelerated. The

prediction,

$$\langle h_{\pm} \rangle = \mp \frac{(1 + \cos \theta)^2 + \phi^T \phi^T \sin^2 \theta \cos^2 \varphi}{1 + \cos^2 \theta + \phi^T \phi^T \sin^2 \theta \cos^2 \varphi} \times \frac{2(\mathcal{E}_{\mu} \rho + g_V) g_A R}{\mathcal{E}_{\mu} + 1} \quad (2.6)$$

is essentially the same as  $A_{1\text{ong}}$  since it does not matter whether the helicity is in the initial or final state. There are additional parity-even contributions to  $\langle h_{\pm} \rangle$  in the form  $\phi^T \phi^T \sin^2 \theta \sin 2\phi$ . These come from higher-order QED corrections<sup>10</sup> and from tiny resonating weak corrections given in Appendix A.

The muons also have transverse spin polarizations given in Appendix A. When only a  $\mu^+$  or  $\mu^-$  is analyzed, such terms are reduced by  $2m_{\mu}/W$  which is 0.02 at  $W=9.46$  GeV. The only one-photon term giving a final spin polarization requires longitudinal beam polarization.

These results show it will be difficult to measure weak effects in  $e^-e^+ \rightarrow \mu^- \mu^+$  on the  $\Upsilon$  resonances. Since the  $\Upsilon$ 's alleged quark is believed to be a member of a doublet, there should be a second quark which can form a heavier resonance, possible in the energy range of PETRA and PEP. The prospects for measuring weak couplings would appear better at larger  $s$ , due to the  $s$  factor in  $R$ . Curiously a narrow resonance probably will not help since the width of the beams  $\sigma_w$  is expected to grow as  $s$ . Thus the combination

$$\mathcal{E}_{\mu} R \sim \Gamma_e^2 / \Gamma \quad (2.7)$$

could remain small compared to the nonresonating terms. For  $\mathcal{E}_{\mu} R$  to be large, either  $W$  must be close to  $M_w$  or else  $\Gamma_e$  must be large.

To anticipate what could be measured at the upper range of PETRA and PEP, suppose there is a resonance at  $W$  near 30 GeV. In the Weinberg-Salam model, the  $R$  terms will be of the order of 10% and the  $R^2$  terms a few percent. The value of  $\delta$  giving the weak correction to  $\mathcal{E}_{\mu}$  defined in Eq. (2.2) is plotted in Fig. 7. The forward-backward asymmetry in Eq. (2.3) is approximately  $-0.07/(\mathcal{E}_{\mu} + 1)$ . The coefficient of the  $\phi^T \phi^T \sin^2 \theta \sin 2\varphi$   $\mathcal{E}_{\mu} \alpha \Gamma / 3\Gamma_e$  term in Eq. (2.1) is 0.19 for  $t$  quarks and 0.05 for  $b$  quarks, but as remarked above,  $\mathcal{E}_{\mu}$  probably will be small. Finally the coefficients  $d_b$  and  $d_r$  in the helicity measurements of Eqs. (2.5) and (2.6) are also shown in Fig. 7.

If storage rings are built with sufficient beam energy for measurements at  $W=M_w$ , the reaction  $e^-e^+ \rightarrow \mu^- \mu^+$  should be dominated by  $W^0$  exchange. The cross section for this is given at the end of Appendix A.

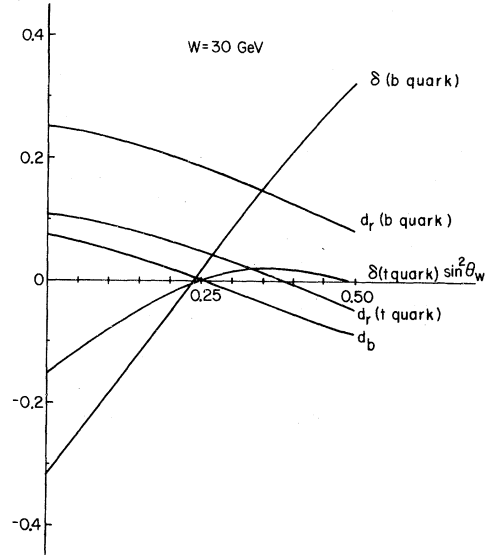


FIG. 7.  $W^0$  corrections to the asymmetry and enhancement from the Weinberg-Salam model at  $W=30$  GeV.

### III. $e^-e^+ \rightarrow \tau^- \tau^+ \rightarrow \mu^\pm$ OR $e^\pm$ + OTHERS

The previous section showed that the less ambiguous measurements of weak terms in  $e^-e^+ \rightarrow \mu^- \mu^+$  require measuring the  $\sin 2\varphi$  term, which is suppressed, or constructing longitudinally polarized beams, which will be difficult, or measuring a final spin, which is hard for muons since their lifetime is too long. The  $\tau$  has a very short lifetime, so its decay measures its spin and thus the weak coupling in Eq. (2.6). Since the lifetime is so short, special steps are needed to ensure that a  $\tau$  pair was produced. One way is to trigger on events with  $\mu^\pm$  and  $e^\pm$  but no hadrons. The rate is reduced by the product of branching ratios,  $B_{\mu} B_e \approx 0.03$ .

The cross section for producing a  $\mu^\pm$  or  $e^\pm$  from  $\tau^- \tau^+$  pairs is gotten by folding the decay distributions for  $\tau \rightarrow l \bar{\nu}_l \nu_\tau$  with the cross section in Appendix A. For the case where the angle  $\Omega$  and energy fraction  $x = E_l/E_{\text{max}}$  of the  $e$  or  $\mu$  are measured, the one-particle inclusive distribution  $d\sigma/d\Omega dx$  is given in Appendix B. Special cases are discussed below.

The forward-backward asymmetry for detecting a  $\mu^\pm$  or  $e^\pm$  from collisions at moderate energy is

$$A_{FB}^\pm = \frac{N_F^\pm - N_B^\pm}{N_F^\pm + N_B^\pm} = F_1 \frac{g_A^2 R}{\mathcal{E}_{\mu} + 1} \mp F_2 \frac{(\mathcal{E}_{\mu} \rho + g_V) g_A R}{\mathcal{E}_{\mu} + 1}. \quad (3.1)$$

Here  $F_1$  and  $F_2$  are functions (specified in Appendix B) of  $x$  and of the speed and decay parameters

of the  $\tau$ . They are plotted in Fig. 8 for the case of  $V-A$  decay at  $W=9.46$  GeV. At  $W=30$  GeV and  $x \gtrsim 0.5$ ,  $F_1 \approx 1.5$  and  $F_2$  is about the same as in Fig. 8. The  $g_A^2 R$  term comes from a  $\cos \theta_\tau$  term in  $\tau^-\tau^+$  production and is the analog of Eq. (2.3). The rest comes from the spin polarization of the  $\tau^\pm$  and is the analog of Eq. (2.6).

Although  $A_{FB}^\pm$  is  $P$  and  $C$  even, the  $F_2$  term is composed of a  $P$ -,  $C$ -odd  $\tau^-\tau^+$  production probability and a  $P$ -,  $C$ -odd  $\tau^\pm$  decay probability. Neither can be simulated by QED so this term is a relatively unambiguous signal for the  $W^0$ . The  $F_1$  term can be simulated by a higher-order QED production followed by the  $P$ -,  $C$ -even  $\tau^\pm$  decay, possibly giving a different  $x$  dependence. One clear way to separate these terms is to measure a for-

ward-backward charge asymmetry

$$A_c = \frac{N_F^- - N_B^- - (N_F^+ - N_B^+)}{N_F^- + N_B^- + N_F^+ + N_B^+} = F_2 \frac{(\mathcal{E}_\mu \rho + g_V) g_A R}{\mathcal{E}_\mu + 1}. \quad (3.2)$$

The magnitudes of these asymmetries at the  $\Upsilon$  can be predicted using the measured  $\Gamma_\rho$  and  $\Gamma$ . The coefficients of  $F_1$  and  $F_2$  in Eq. (3.1) should be  $-0.003$  and  $+0.003$ . Measuring  $A_c$ , which is roughly proportional to  $\rho$ , would require an integrated luminosity of  $10^6/(B_\mu B_\rho \text{ nb})$ . At 30 GeV, the coefficients should be  $-0.045/(1 + \mathcal{E}_\mu)$  and 0 for a  $t$  quark. Measuring  $A_{FB}^\pm$  would require  $2 \times 10^4 \times (1 + \mathcal{E}_\mu)/(B_\mu B_\rho \text{ nb})$ .

#### IV. $e^-e^+ \rightarrow e^-e^+$

The cross section for Bhabha scattering is given in Appendix C. For the case where the beams are unpolarized or transversely polarized, and  $s$  is small compared to  $M_W^2$ , the result is

$$\begin{aligned} \frac{d\sigma}{d\Omega} = \frac{\alpha^2}{4s} & \left\{ \mathcal{E}_e^0(1+z^2) + \frac{(3+z^2)^2}{(1-z)^2} + [\mathcal{E}_e^0(1-z^2) - (1+z)^2] \mathcal{P}_+^T \mathcal{P}_+^T \cos 2\phi \right. \\ & - \frac{s}{e^2 M_W^2} \left[ \mathcal{E}_e^0 4\rho g_V(1+z^2) - 3g_V^2 \frac{(1+z)(3+z^2)}{1-z} - g_A^2 \frac{(1+z)(-5+8z+z^2)}{1-z} \right] \\ & - \frac{s}{e^2 M_W^2} \mathcal{P}_-^T \mathcal{P}_+^T \cos 2\phi [\mathcal{E}_e^0 4\rho g_V(1-z^2) + g_V^2(1+z)(1-3z) + g_A^2(1+z)(3-z)] \\ & \left. - \frac{s}{e^2 M_W^2} \mathcal{P}_-^T \mathcal{P}_+^T \sin 2\phi (1-z^2) \mathcal{E}_e^0 \frac{\alpha \Gamma}{3\Gamma_e} 2\rho g_A \right\}. \end{aligned} \quad (4.1)$$

Here  $z = \cos \theta$  and  $\mathcal{E}_e^0$  is given in Eq. (1.3). The first line is the QED contribution. The factors  $-s/e^2 M_W^2$  come from  $R$  or from  $\bar{R}$  which results from  $t$ -channel  $W^0$  exchanges.

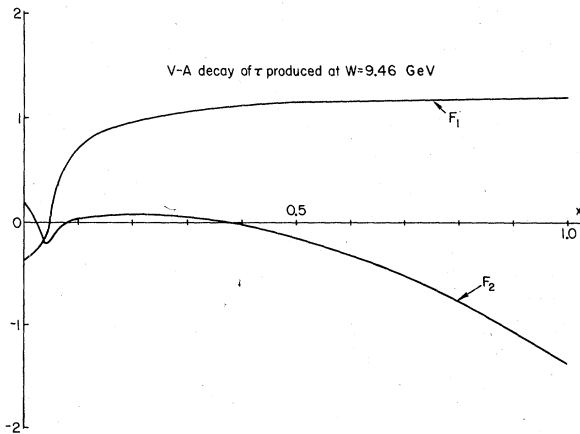


FIG. 8. Kinematic functions for the one-particle inclusive cross section from the decay of a  $\tau$  of mass 1.78 GeV produced at  $W=9.46$  GeV.

The resonant terms (containing  $\mathcal{E}_e^0$ ) resemble those for  $e^-e^+ \rightarrow \mu^-\mu^+$  in Eq. (2.1) but one of the  $\sin 2\phi$  terms there does not occur here leaving a larger  $\sin 2\phi$  signal for this reaction.

It does not seem convenient to replace  $\mathcal{E}_e^0$  with an observed  $\mathcal{E}_e$  normalized relative to the nonresonating background as in Eq. (2.2) for several reasons. The latter has a very different (forward peaked)  $\theta$  distribution. Also it has very large radiative corrections.<sup>11</sup>

To illustrate the magnitude of  $W^0$  corrections, rearrange the unpolarized case of Eq. (4.1) as

$$\frac{d\sigma}{d\Omega} = \frac{\alpha^2}{4s} \left[ \mathcal{E}_e^0(1+z^2)(1+\delta_r) + \frac{(3+z^2)^2}{(1-z)^2}(1+\delta_b) \right]. \quad (4.2)$$

The  $W^0$  corrections are in  $\delta_r$  and  $\delta_b$ . The resonant correction is  $\delta_r = 4\rho g_V R$ . The shape of the background correction  $\delta_b$  versus  $\cos \theta$  for the Weinberg-Salam model at  $W=9.4$  GeV is shown in Fig. 9. The shape at  $W=28$  GeV is shown in Ref. 3.

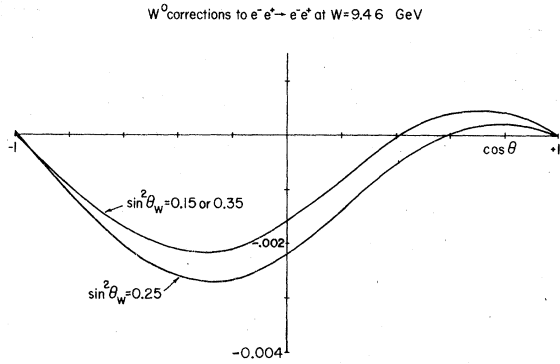


FIG. 9.  $W^0$  correction to the differential cross section for Bhabha scattering.

#### ACKNOWLEDGMENT

I wish to thank Aidan McDonald, Hartmut Sadrozinski, Robert Shrock, and Sam Treiman for help.

#### APPENDIX A: $e^-e^+ \rightarrow F^-F^+$

The differential cross section for annihilations producing spin- $\frac{1}{2}$  particle pairs is given. The result was applied to the production of  $\mu^-\mu^+$  and  $\tau^-\tau^+$  in Sec. II and Appendix B.

The kinematic notation used is that of Ref. 4. Specifically, the momenta of the  $e^\pm$  and  $F^\pm$  in the center-of-momentum frame, or laboratory frame, illustrated in Fig. 10, are

$$k_\pm^\alpha = E(1, 0, 0, \mp 1), \quad (\text{A1})$$

$$k_\pm'^\alpha = E(1, \mp \beta \sin \theta \cos \varphi, \mp \beta \sin \theta \sin \varphi, \mp \beta \cos \theta).$$

The mass of the electron has been dropped and  $\beta = (1 - 1/\gamma^2)^{1/2}$  with  $\gamma = E/M_F = W/2M_F = \sqrt{s}/2M_F$ .

The spin polarizations of the  $e^\pm$  beams are

$$\vec{\phi}_\pm = (\phi_\pm^T \cos \varphi_\pm, \phi_\pm^T \sin \varphi_\pm, \phi_\pm^L), \quad (\text{A2})$$

with  $\pm \phi_\pm^L$  the helicities of the  $e^\pm$  beams. In the case of transverse polarization  $\phi_\pm^T$  are expected to relax to  $\pm 0.924$ , and  $\varphi_\pm$  and  $\phi_\pm^L$  are zero.

The beam polarizations occur in the cross section only in the forms

$$\begin{aligned} U &= 1 + \phi_-^L \phi_+^L, \\ T_c &= \phi_-^T \phi_+^T \cos(2\varphi - \varphi_+ - \varphi_-), \\ T_s &= \phi_-^T \phi_+^T \sin(2\varphi - \varphi_+ - \varphi_-), \\ L &= \phi_-^L + \phi_+^L. \end{aligned} \quad (\text{A3})$$

These would vanish if  $\phi_-^L = -\phi_+^L = \pm 1$ , due to the assumption of spin 1 for all the virtual particles.

The final  $F^\pm$  are assumed to have spin polarizations  $\vec{S}_\pm$  in the rest frames, which are oriented so

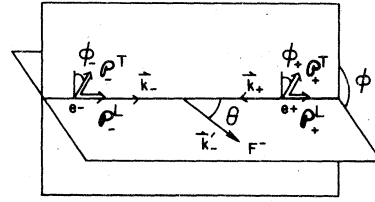


FIG. 10. Definitions of kinematic variables.

their  $z$  axes are in the direction of  $\vec{k}_-$ , their  $x$  axes are in the scattering plane (containing  $\vec{k}_+$  and  $\vec{k}'_+$ ), and their  $y$  axes are in the direction  $\vec{k}_- \times \vec{k}'_+$ . With this choice, the helicities of the  $F^\pm$  in the center-of-momentum frame are  $\pm S_\pm^z$ .

The couplings of the  $W^0$  and the resonances are assumed to have the forms

$$\begin{aligned} \langle 0 | J_\alpha^W | e^- e^+ \rangle &= \bar{v}(k_+, \phi_+) \gamma_\alpha (g_V + g_A \gamma_5) u(k_-, \phi_-), \\ \langle F^- F^+ | J_\alpha^W | 0 \rangle &= \bar{u}(k'_-, s_-) \gamma_\alpha (G_V + G_A \gamma_5) v(k'_+, s_+), \end{aligned} \quad (\text{A4})$$

$$\langle 0 | J_\alpha^W | \Upsilon_i \rangle = \frac{e_\alpha}{(2\pi)^{3/2}} f_{W,i} M_i^2,$$

$$\langle 0 | J_\alpha^{\text{em}} | \Upsilon_i \rangle = \frac{e_\alpha}{(2\pi)^{3/2}} f_{Q,i} M_i^2.$$

The widths for the decay of a resonance to  $e^-e^+$  or  $F^-F^+$  in the tree approximation (Fig. 2) are

$$\Gamma_e = \frac{e^2}{12\pi} f_{Q,i}^2 M_i [(1 + \rho g_V R)^2 + (\rho g_A R)^2], \quad (\text{A5})$$

$$\Gamma_F = \frac{e^2}{12\pi} f_{Q,i}^2 M_i [(1 + \rho G_V R)^2 + (\rho \beta G_A R)^2].$$

Here  $\rho = ef_{W,i}/f_{Q,i}$  and  $R = s[e^2(s - M_W^2)]^{-1}$  with  $s = M_i^2$ .

In the Weinberg-Salam model, the  $W^0$  couplings to charged leptons are

$$g_V = G_V = \frac{e}{2 \sin 2\theta_W} (4 \sin^2 \theta_W - 1), \quad (\text{A6})$$

$$g_A = G_A = \frac{e}{2 \sin 2\theta_W}.$$

The ratio  $\rho$  for a  $t$  ( $b$ ) quark with weak isospin  $\tau_L = +\frac{1}{2}$  ( $-\frac{1}{2}$ )

$$\rho = \left( \frac{e}{Q} \right) \frac{e}{2 \sin 2\theta_W} \left( 4 \frac{Q}{e} \sin^2 \theta_W + 2\tau_L \right). \quad (\text{A7})$$

These are plotted in Fig. 5.

The amplitudes for  $e^-e^+ \rightarrow F^-F^+$  in the tree approximation are shown in Fig. 4. They are proportional to

$$\begin{aligned} vV &= R_Q + R_{QW} (g_V + G_V) R + R_W g_V G_V R^2 + 1 + g_V G_V R, \\ vA &= (R_{QW} + R_W g_V R + g_V) \beta G_A R, \\ aV &= (R_{QW} + R_W G_V R + G_V) g_A R, \\ aA &= (R_W R + 1) \beta g_A G_A R, \end{aligned} \quad (\text{A8})$$

where  $R_Q$ ,  $R_{QW}$ , and  $R_W$  are sums over all 1<sup>-</sup> resonances contributing:

$$\begin{aligned} R_Q &= \sum_i \frac{f_{Q,i}^2 M_i^4}{s(s-M_i^2)}, \\ R_{WQ} &= \sum_i \frac{ef_{Q,i}f_{W,i}M_i^4}{s(s-M_i^2)}, \\ R_W &= \sum_i \frac{e^2 f_{W,i}^2 M_i^4}{s(s-M_i^2)}. \end{aligned} \quad (A9)$$

Note that the  $R_W$  terms come from the diagram in Fig. 4 with two virtual  $W^0$ 's. They contribute to the same order as the square of the amplitude of the last diagram.

The amplitudes in Eq. (A8) occur in the cross section in the following combinations:

$$\begin{aligned} \mathcal{L}_{1,j,k} &= |vV|^2 + \epsilon_j |aV|^2 + \epsilon_k |vA|^2 + \epsilon_j \epsilon_k |aA|^2, \\ \mathcal{L}_{2,j} &= 2 \operatorname{Re}[vV(aV)^* + \epsilon_j vA(aA)^*], \\ \mathcal{L}_{3,j} &= 2 \operatorname{Re}[vV(vA)^* + \epsilon_j aV(aA)^*], \end{aligned}$$

$$\mathcal{L}_{4,j} = 2 \operatorname{Re}[vV(aA)^* + \epsilon_j aV(vA)^*], \quad (A10)$$

$$\mathcal{L}_{5,j} = 2 \operatorname{Im}[vV(aV)^* + \epsilon_j vA(aA)^*],$$

$$\mathcal{L}_{6,j} = 2 \operatorname{Im}[vV(vA)^* + \epsilon_j aV(aA)^*],$$

$$\mathcal{L}_{7,j} = 2 \operatorname{Im}[vV(aA)^* + \epsilon_j vA(aV)^*],$$

with

$$\epsilon_j = \begin{cases} +1, & j = + \\ 0, & j = 0 \\ -1, & j = - \end{cases}.$$

When the weak couplings of the  $F$  and  $e$  are equal,  $vA = \beta aV$  so that  $\mathcal{L}_{2,j} = \beta \mathcal{L}_{3,j}$  and  $\mathcal{L}_{5,j} = \beta \mathcal{L}_{6,j}$  (neglecting  $1/\gamma^2$  corrections to  $R^2$  terms). The terms which depend on  $\epsilon_j$  or  $\epsilon_k$  are proportional to  $R^2$ , i.e., are purely weak and can be neglected unless  $s$  is large.

The cross section when the spin of either the  $F^-$  or  $F^+$  is observed is

$$\begin{aligned} \frac{d\sigma}{d\Omega} &= \frac{\alpha^2 \beta}{8s} \left\{ U \left[ (1 + \cos^2 \theta) \mathcal{L}_{1,+,+} + \frac{\sin^2 \theta}{\gamma^2} \mathcal{L}_{1,+,0} + 2 \cos \theta \mathcal{L}_{4,+} \right] + T_c \sin^2 \theta \left( \mathcal{L}_{1,-,+} - \frac{1}{\gamma^2} \mathcal{L}_{1,-,0} \right) \right. \\ &+ T_s \sin^2 \theta \left( \mathcal{L}_{5,+} - \frac{1}{\gamma^2} \mathcal{L}_{5,0} \right) + L \left[ (1 + \cos^2 \theta) \mathcal{L}_{2,+,+} + \frac{\sin^2 \theta}{\gamma^2} \mathcal{L}_{2,0} + 2 \cos \theta \mathcal{L}_{3,+} \right] \\ &+ S_+^z [2 \cos \theta (U \mathcal{L}_{2,+,+} + L \mathcal{L}_{1,+,+}) + (1 + \cos^2 \theta) (U \mathcal{L}_{3,+,+} + L \mathcal{L}_{4,+,+}) + \sin^2 \theta (T_c \mathcal{L}_{3,-,+} + T_s \mathcal{L}_{7,+,+})] \\ &- S_+^y \frac{\sin \theta}{\gamma} [2 (U \mathcal{L}_{2,0} + L \mathcal{L}_{1,+,0}) + \cos \theta (U \mathcal{L}_{3,+} - T_c \mathcal{L}_{3,-} + L \mathcal{L}_{4,+} - T_s \mathcal{L}_{7,+,+})] \\ &\left. - S_+^x \frac{\sin \theta}{\gamma} [T_s \mathcal{L}_{3,-} + U \mathcal{L}_{7,-} - T_c \mathcal{L}_{7,+,+} + L \mathcal{L}_{6,+,+}] \right\}. \end{aligned} \quad (A11)$$

In the more general case where the spins of both  $F^-$  and  $F^+$  are observed, the cross section is

$$\begin{aligned} \frac{16s}{\alpha^2 \beta} \frac{d\sigma}{d\Omega} &= [U(1 + \cos^2 \theta)(1 + S_-^z S_+^z) + L2 \cos \theta (S_-^z + S_+^z)] \mathcal{L}_{1,+,+} + \sin^2 \theta [T_c(1 + S_-^z S_+^z) \mathcal{L}_{1,-,+} + U(S_-^x S_+^x - S_-^y S_+^y) \mathcal{L}_{1,+,+}] \\ &+ [T_c(1 + \cos^2 \theta)(S_-^x S_+^x - S_-^y S_+^y) - T_s 2 \cos \theta (S_-^x S_+^x + S_-^y S_+^y)] \mathcal{L}_{1,-,-} \\ &+ \frac{\sin \theta}{\gamma} \left\{ -2[L(S_-^x + S_+^x) + U \cos \theta (S_-^x S_+^x + S_-^y S_+^y)] + U \frac{\sin \theta}{\gamma} (1 - S_-^z S_+^z + S_-^x S_+^x + S_-^y S_+^y) \right\} \mathcal{L}_{1,+,0} \\ &+ \frac{\sin \theta}{\gamma} \left\{ 2[T_c(S_-^x S_+^x + S_-^y S_+^y) - T_s(S_-^y S_+^y + S_-^z S_+^z)] - T_c \frac{\sin \theta}{\gamma} (1 - S_-^z S_+^z + S_-^x S_+^x + S_-^y S_+^y) \right\} \mathcal{L}_{1,-,0} \\ &+ [L(1 + \cos^2 \theta)(1 + S_-^z S_+^z) + U2 \cos \theta (S_-^z + S_+^z)] \mathcal{L}_{2,+,+} + L \sin^2 \theta (S_-^x S_+^x - S_-^y S_+^y) \mathcal{L}_{2,-,-} \\ &+ \frac{\sin \theta}{\gamma} \left\{ -2[U(S_-^x + S_+^x) + L \cos \theta (S_-^x S_+^x + S_-^y S_+^y) + L \frac{\sin \theta}{\gamma} (1 - S_-^z S_+^z + S_-^x S_+^x + S_-^y S_+^y)] \right\} \mathcal{L}_{2,0} \\ &+ \left\{ L2 \cos \theta (1 + S_-^z S_+^z) + U(1 + \cos^2 \theta)(S_-^z + S_+^z) - \frac{\sin \theta}{\gamma} [U \cos \theta (S_-^x + S_+^x) + L(S_-^x S_+^x + S_-^y S_+^y)] \right\} \mathcal{L}_{3,+,+} \\ &+ \sin \theta \left\{ T_c \sin \theta (S_-^z + S_+^z) + \frac{1}{\gamma} [T_c \cos \theta (S_-^x + S_+^x) - T_s(S_-^y + S_+^y)] \right\} \mathcal{L}_{3,-,-} \\ &+ \left\{ U2 \cos \theta (1 + S_-^z S_+^z) + L(1 + \cos^2 \theta)(S_-^z + S_+^z) - \frac{\sin \theta}{\gamma} [L \cos \theta (S_-^x + S_+^x) + U(S_-^x S_+^x + S_-^y S_+^y)] \right\} \mathcal{L}_{4,+,+} \end{aligned}$$

$$\begin{aligned}
& + \left\{ T_c 2 \cos \theta (S_-^x S_+^x - S_-^y S_+^y) - T_s (1 + \cos^2 \theta) (S_-^x S_+^y + S_-^y S_+^x) \right. \\
& \quad \left. + \frac{\sin \theta}{\gamma} [T_c (S_-^x S_+^z + S_-^z S_+^x) - T_s \cos \theta (S_-^y S_+^z + S_-^z S_+^y)] \right\} \mathfrak{L}_{4,-} \\
& + T_s \sin^2 \theta (1 + S_-^z S_+^z) \mathfrak{L}_{5,+} + [T_c 2 \cos \theta (S_-^x S_+^y + S_-^y S_+^x) + T_s (1 + \cos^2 \theta) (S_-^x S_+^x - S_-^y S_+^y)] \mathfrak{L}_{5,-} \\
& + \frac{\sin \theta}{\gamma} \left\{ 2 [T_c (S_-^y S_+^z + S_-^z S_+^y) + T_s \cos \theta (S_-^x S_+^z + S_-^z S_+^x)] - T_s \frac{\sin \theta}{\gamma} (1 - S_-^z S_+^z + S_-^x S_+^x + S_-^y S_+^y) \right\} \mathfrak{L}_{5,0} \\
& + \sin \theta \left\{ U \sin \theta (S_-^x S_+^y + S_-^y S_+^x) - \frac{1}{\gamma} [L (S_-^y + S_+^y) + U \cos \theta (S_-^y S_+^z + S_-^z S_+^y)] \right\} \mathfrak{L}_{6,+} \\
& + \left\{ T_c (1 + \cos^2 \theta) (S_-^x S_+^y + S_-^y S_+^x) + T_s 2 \cos \theta (S_-^x S_+^z - S_-^y S_+^z) \right. \\
& \quad \left. + \frac{1}{\gamma} [T_c \cos \theta (S_-^y S_+^z + S_-^z S_+^y) + T_s (S_-^x S_+^z + S_-^z S_+^x)] \right\} \mathfrak{L}_{6,-} \\
& + \sin \theta \left\{ T_s \sin \theta (S_-^z + S_+^z) + \frac{1}{\gamma} [T_c (S_-^y + S_+^y) + T_s \cos \theta (S_-^x + S_+^x)] \right\} \mathfrak{L}_{7,+} \\
& + \sin \theta \left\{ L \sin \theta (S_-^x S_+^y + S_-^y S_+^x) - \frac{1}{\gamma} [U (S_-^y + S_+^y) + L \cos \theta (S_-^y S_+^z + S_-^z S_+^y)] \right\} \mathfrak{L}_{7,-} . \tag{A12}
\end{aligned}$$

The discrete symmetries of the terms in these cross sections can be read off from Eq. (A10). The terms with  $\mathfrak{L}_{1,j,k}$ ,  $\mathfrak{L}_{4,j}$ , and  $\mathfrak{L}_{7,j}$  are even under  $P$  and  $C$  whereas the rest are odd.

The formalism discussed so far can be applied to cases of overlapping resonances. In the case where the storage ring is tuned to one resonance without overlapping another, then  $M_i = M_0 - i \Gamma/2$  gives

$$\begin{aligned}
R_Q &= \frac{f_Q^2 m_0^4}{s(s - m_0^2 + iM_0\Gamma)} , \\
R_{QW} &= \rho R_Q , \\
R_W &= \rho^2 R_Q ,
\end{aligned} \tag{A13}$$

for Eq. (A9). In this case the expressions for the  $\mathfrak{L}$ 's contain pole terms proportional to

$$\begin{aligned}
\mathfrak{P} &= \left( \frac{f_Q^2 m_0^4}{s} \right)^2 \frac{1}{(s - m_0^2)^2 + m_0^2 \Gamma^2} , \\
\mathfrak{D} &= \left( \frac{f_Q^2 m_0^4}{s} \right) \frac{s - m_0^2}{(s - m_0^2)^2 + m_0^2 \Gamma^2} , \\
\mathfrak{Q} &= \left( \frac{f_Q^2 m_0^4}{s} \right) \frac{m_0 \Gamma}{(s - m_0^2)^2 + m_0^2 \Gamma^2} ,
\end{aligned} \tag{A14}$$

and background terms. Explicitly they are

$$\begin{aligned}
\mathfrak{L}_{1,j,k} &= \{ 1 + 2\rho(g_V + G_V)R + \rho^2(g_V^2 + 4g_V G_V + G_V^2 + \epsilon_j g_A^2 + \epsilon_k \beta^2 G_A^2)R^2 \} \mathfrak{P} \\
& \quad + 2\{ 1 + [\rho(g_V + G_V) + g_V G_V]R + \rho[(\rho + g_V + G_V)g_V G_V + \epsilon_j g_A^2 G_V + \epsilon_k \beta^2 g_V G_A^2]R^2 \} \mathfrak{D} \\
& \quad + 1 + 2g_V G_V R + (g_V^2 + \epsilon_j g_A^2)(G_V^2 + \epsilon_k \beta^2 G_A^2)R^2 , \\
\mathfrak{L}_{2,j} &= 2\rho g_A R [1 + \rho(g_V + 2G_V)R] \mathfrak{P} + 2g_A R \{ \rho + G_V + \rho[(\rho + 2g_V + G_V)G_V + \epsilon_j \beta^2 G_A^2]R \} \mathfrak{D} \\
& \quad + 2g_A R [G_V + g_V(G_V^2 + \epsilon_j \beta^2 G_A^2)R] , \\
\mathfrak{L}_{3,j} &= 2\beta \rho G_A R [1 + \rho(2g_V + G_V)R] \mathfrak{P} + 2\beta G_A R \{ \rho + g_V + \rho[(\rho + 2G_V + g_V)g_V + \epsilon_j g_A^2]R \} \mathfrak{D} \\
& \quad + 2\beta G_A R [g_V + G_V(g_V^2 + \epsilon_j g_A^2)R] , \\
\mathfrak{L}_{4,j} &= 2\beta \rho^2 g_A G_A R^2 (1 + \epsilon_j) \mathfrak{P} + 2\beta g_A G_A R \{ 1 + \rho[\rho + (1 + \epsilon_j)(g_V + G_V)]R \} \mathfrak{D} \\
& \quad + 2\beta g_A G_A R [1 + (1 + \epsilon_j)g_V G_V R] , \\
\mathfrak{L}_{5,j} &= 2g_A R \{ \rho - G_V + \rho[(\rho - G_V)G_V - \epsilon_j \beta^2 G_A^2]R \} \mathfrak{Q} , \\
\mathfrak{L}_{6,j} &= 2\beta G_A R \{ \rho - g_V + \rho[(\rho - g_V)g_V - \epsilon_j g_A^2]R \} \mathfrak{Q} , \\
\mathfrak{L}_{7,j} &= 2\beta g_A G_A R \{ -1 + \rho[\rho - g_V - G_V + \epsilon_j(g_V - G_V)R] \} \mathfrak{Q} .
\end{aligned} \tag{A15}$$



When the cross section with these  $\mathcal{L}$ 's is radiatively corrected and folded with  $\sigma_w$ , as discussed in Sec. I, the  $\mathcal{O}$  terms are enhanced by  $\mathcal{E}$  over the nonresonating terms. The  $\mathcal{D}$  terms average to zero unless the storage ring is tuned slightly away from the pole. The  $\mathcal{Q}$  terms are proportional to the  $\mathcal{O}$  terms scaled down by

$$\frac{\mathcal{Q}}{\mathcal{O}} = \frac{\Gamma}{f_Q^2 m_0}. \quad (\text{A16})$$

The value of  $f_Q^2$  can be expressed in terms of  $\Gamma_e$  or  $\Gamma_F$  using Eq. (A5).

The QED expression for  $\mathcal{E}$  is given in Eq. (1.2). The  $W^0$  corrections are given by  $\mathcal{L}_{1,j,k}$  (which are the only terms in the total cross section). With terms of the order of  $1/\gamma^2$  dropped from the  $R^2$  terms, the  $W^0$  corrections are

$$\mathcal{E} = \mathcal{E}^0(1 + \delta), \quad 1 + \delta = \frac{1 + 2\rho(g_V + G_V)R + \rho^2(g_V^2 + 4g_V G_V + G_V^2 + g_A^2 + G_A^2)R^2}{1 + 2g_V G_V R + (g_V^2 + g_A^2)(G_V^2 + G_A^2)R^2}. \quad (\text{A17})$$

This is proportional to the product  $\Gamma_e \Gamma_F$  in Eq. (A5) (to the order of  $R^2$ ). The denominator resulted from normalizing  $\mathcal{E}$  to the nonresonant background. Predictions for  $\delta$  are shown in Figs. 6 and 7.

When  $W$  is close to  $M_w$ , the cross section is given by Eq. (A11) or (A12) with the following  $\mathcal{L}$ 's:

$$\begin{aligned} \mathcal{L}_{1,j,k} &= (g_V^2 + \epsilon_j g_A^2)(G_V^2 + \epsilon_k \beta^2 G_A^2) |R|^2 \\ &\quad + 2g_V G_V \text{Re}(R) + 1, \\ \mathcal{L}_{2,j} &= 2g_A g_V (G_V^2 + \epsilon_j \beta^2 G_A^2) |R|^2 + 2g_A G_V \text{Re}(R), \\ \mathcal{L}_{3,j} &= 2\beta g_A G_V (g_V^2 + \epsilon_j g_A^2) |R|^2 + 2\beta g_V G_A \text{Re}(R), \\ \mathcal{L}_{4,j} &= 2\beta g_V g_A G_V G_A (1 + \epsilon_j) |R|^2 + 2\beta g_A G_A \text{Re}(R), \\ \mathcal{L}_{5,j} &= 2g_A G_V \text{Im}(R^*), \\ \mathcal{L}_{6,j} &= 2\beta g_V G_A \text{Im}(R^*), \\ \mathcal{L}_{7,j} &= 2\beta g_A G_A \text{Im}(R^*). \end{aligned} \quad (\text{A18})$$

The partial widths of the  $W^0$ ,

$$\begin{aligned} \Gamma_e &= \frac{M_w}{12\pi} (g_V^2 + g_A^2), \\ \Gamma_F &= \frac{M_w}{12\pi} (G_V^2 + \beta^2 G_A^2), \end{aligned}$$

suggest that the total width  $\Gamma$  is about 1 GeV. If this is large compared to  $\sigma_w$ , the cross section at  $M_w^2$  is

$$\sigma(M_w^2) = \left(\frac{\Gamma}{M_w}\right)^6 \frac{12\pi \Gamma_e \Gamma_F}{M_w^2 \Gamma^2}. \quad (\text{A19})$$

The  $\text{Re}(R)$  terms in Eq. (A18) will average to zero at  $M_w^2$  and the  $\text{Im}(R)$  terms should be negligible since apparently

$$\frac{\text{Im}(R^*)}{|R|^2} = \frac{e^2 \Gamma}{M_w} \simeq 10^{-3}. \quad (\text{A20})$$

#### APPENDIX B: THE DISTRIBUTION FROM $\tau \rightarrow l\nu\bar{\nu}$

The general one-particle inclusive distribution for the reaction

$$e^- e^+ \rightarrow \tau^- \tau^+ \rightarrow l\nu\bar{\nu} X \quad (\text{B1})$$

is given here. Applications were discussed in Sec. III.

Since  $\tau$  is very narrow, it is produced on its mass shell. Then the distribution of the decays can be calculated by folding the  $\tau^- \tau^+$  production cross section in Eq. (A12) with the decay rates  $\Gamma_-$  and  $\Gamma_+$  of the  $\tau^-$  and  $\tau^+$ , and integrating over the unobserved measurables.<sup>12</sup>

Using the appropriate  $\Gamma_{\pm}$  for whatever decay is observed, this procedure gives distributions such as the angle between two decay products, or the energies of two decay products. As an example, in the following the result is given for the case where the momentum of one lepton,  $l^{\pm}$  from  $\tau^{\pm}$ , is observed and the other  $\tau^{\pm}$  decays to any specified state are used as a signature (to guarantee  $\tau^- \tau^+$  production).

The rate  $\Gamma_{\pm}$  for the decay  $\tau^{\pm} \rightarrow l^{\pm} \nu \bar{\nu}$  implied by the general four-fermion Lagrangian is

$$\frac{p^0}{\Gamma_{\pm}} \frac{d^3 \Gamma_{\pm}}{d^3 \mathbf{p}} = \frac{12}{M_{\tau}^2 \pi} \left[ y G(y, \rho) \mp \xi \frac{2}{M_{\tau}} (p \cdot S_{\pm}) G(y, \delta) \right] \quad (\text{B2})$$

when the mass of  $l$  is neglected. Here  $p$  is the momentum of  $l$ . Also

$$y = \frac{2}{M_{\tau}^2} p \cdot k'_{\pm} \quad (\text{B3})$$

and

$$G(y, \rho) = 1 - y + \frac{2}{3} \rho \left( \frac{4}{3} y - 1 \right)$$

with  $k'_{\pm}$  the momentum of the  $\tau$ . The parameters  $\rho$ ,  $\delta$ , and  $\xi$  depend on the mix of  $V$ ,  $A$ ,  $S$ ,  $P$ , or  $T$  of the decay.<sup>13</sup>

The one-particle inclusive distribution is

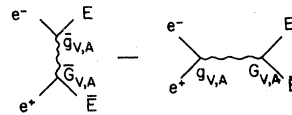


FIG. 11. Form of the Bhabha-type amplitudes.

$$\begin{aligned}
\frac{12s}{\alpha^2 \beta B_l B_s} \frac{d\sigma^+}{d\Omega dx} = & U \left\{ 2 \left( 2\mathcal{L}_{1,+} + \frac{1}{\gamma^2} \mathcal{L}_{1,+0} \right) A(x, \rho) + (3 \cos^2 \theta - 1) \mathcal{L}_{1,+} - \frac{1}{\gamma^2} \mathcal{L}_{1,+0} B(x, \rho) \right. \\
& \left. + 6 \cos \theta \mathcal{L}_{4,+} [\beta^2 C(x, \rho) - D(x, \rho)] \right\} \\
& \pm \xi U \mathcal{L}_{3,+} \left\{ (3 \cos^2 \theta - 1) \beta^2 [A(x, \delta) - B(x, \delta)] - 3(1 + \cos^2 \theta) D(x, \delta) \right\} \\
& \pm \xi U 6 \cos \theta \left[ \mathcal{L}_{2,+} A(x, \delta) - \left( \mathcal{L}_{2,+} - \frac{1}{\gamma^2} \mathcal{L}_{2,0} \right) C(x, \delta) \right] \\
& + 3 T_c \sin^2 \theta \left\{ \left( \mathcal{L}_{1,-} - \frac{1}{\gamma^2} \mathcal{L}_{1,-0} \right) B(x, \rho) \pm \xi \mathcal{L}_{3,-} [\beta^2 A(x, \delta) - \beta^2 B(x, \delta) - D(x, \delta)] \right\} \\
& + 3 T_s \sin^2 \theta \left\{ \left( \mathcal{L}_{5,+} - \frac{1}{\gamma^2} \mathcal{L}_{5,0} \right) B(x, \rho) \pm \xi \mathcal{L}_{7,+} [\beta^2 A(x, \delta) - \beta^2 B(x, \delta) - D(x, \delta)] \right\} \\
& + L \left\{ 2 \left( 2\mathcal{L}_{2,+} + \frac{1}{\gamma^2} \mathcal{L}_{2,0} \right) A(x, \rho) + (3 \cos^2 \theta - 1) \left( \mathcal{L}_{2,+} - \frac{1}{\gamma^2} \mathcal{L}_{2,0} \right) B(x, \rho) \right. \\
& \left. + 6 \cos \theta \mathcal{L}_{3,+} [\beta^2 C(x, \rho) - D(x, \rho)] \right\} \\
& \pm \xi L 6 \cos \theta \left\{ \mathcal{L}_{1,+} A(x, \delta) - \left( \mathcal{L}_{1,+} - \frac{1}{\gamma^2} \mathcal{L}_{1,+0} \right) C(x, \delta) \right\} \\
& \pm \xi L \mathcal{L}_{4,+} \left\{ (3 \cos^2 \theta - 1) \beta^2 [A(x, \delta) - B(x, \delta)] - 3(1 + \cos^2 \theta) D(x, \delta) \right\}. \tag{B4}
\end{aligned}$$

Here,  $B_l$  and  $B_s$  are the branching ratios of the decays to  $l$  and to the signature. The angle  $\Omega$  is the direction of  $l$ , and the energy fraction  $x$  is defined by

$$x = \frac{p^0}{p_{\max}^0} = \frac{2p^0}{(1+\beta)E}. \tag{B5}$$

The  $\mathcal{L}$ 's are given in Appendix A. The functions  $A$ ,  $B$ , and  $C$  of the  $\tau$  decay parameters (and speed) are defined in Ref. 14, and  $D$  is defined in Ref. 4.

The functions  $F_1$  and  $F_2$  used in Sec. III are

$$F_1 = \frac{3\beta}{3-\beta^2} \left( \frac{\beta^2 C - D}{A} \right), \quad F_2 = \frac{3}{3-\beta^2} \xi \left( \frac{\beta^2 C - A}{A} \right). \tag{B6}$$

Their values for  $V-A$  decays at  $W=9.4$  GeV are shown in Fig. 8. When  $\gamma=W/2m_\tau$  is large,  $F_1 = \frac{3}{2}$ , and the shape of  $2F_2/3$  has been given in Figs. 1 and 2 of Ref. 4.

In principle,  $\mu$ - $\tau$  universality of neutral-current couplings can be tested. One test is to compare  $L_{2,j}$  with  $L_{3,j}$ . These are measured by a  $\cos \theta$  and a  $T_c \sin^2 \theta$  term, respectively, in Eq. (B4).

#### APPENDIX C: $e^-e^+ \rightarrow E\bar{E}$

The general Bhabha-type cross section is given here. The case  $e^-e^+ \rightarrow e^-e^+$  was discussed in Sec. IV, and  $e^-e^+ \rightarrow E^0\bar{E}^0$  is discussed in the end of this appendix.

The tree amplitudes are those with  $s$ -channel exchanges, illustrated in Fig. 4, and their  $t$ -channel analogs. To include both reactions, the couplings are kept distinct, in the form of Fig. 11. It is convenient to combine the couplings as  $vV$ , etc., defined in Eq. (A8), and their  $t$ -channel analogs with

$$s \rightarrow t = (k'_- - k_-)^2 = -s(1 - \cos \theta)/2. \tag{C1}$$

These amplitudes occur in the general cross section in the combinations

$$\begin{aligned}
\mathfrak{A}_1 &= \bar{\mathcal{L}}_{1,+} - \bar{\mathcal{L}}_{4,+} = |\bar{v}\bar{V} - \bar{a}\bar{A}|^2 + |\bar{a}\bar{V} - \bar{v}\bar{A}|^2, \\
\mathfrak{A}_2 &= \mathcal{L}_{1,+} - \mathcal{L}_{4,+} = |vV - aA|^2 + |aV - vA|^2, \\
\mathfrak{A}_3 &= |vV + aA + \bar{v}\bar{V} + \bar{a}\bar{A}|^2 + |aV + vA + \bar{a}\bar{V} + \bar{v}\bar{A}|^2, \\
\mathfrak{A}_4 &= 2 \operatorname{Re}[(vV + aA + \bar{v}\bar{V} + \bar{a}\bar{A})^*(vV - aA) + (vA + aV + \bar{v}\bar{A} + \bar{a}\bar{V})^*(vA - aV)], \\
\mathfrak{A}_5 &= 2 \operatorname{Im}[(vA + aV - \bar{v}\bar{A} - \bar{a}\bar{V})^*(vV - aA) + (vV + aA - \bar{v}\bar{V} - \bar{a}\bar{A})^*(vA - aV)], \\
\mathfrak{A}_6 &= 2 \operatorname{Re}[(vV + aA + \bar{v}\bar{V} + \bar{a}\bar{A})^*(vA + aV + \bar{v}\bar{A} + \bar{a}\bar{V})], \\
\mathfrak{A}_7 &= \mathcal{L}_{2,+} - \mathcal{L}_{3,+} = 2 \operatorname{Re}[(vV - aA)^*(aV - vA)], \\
\mathfrak{A}_8 &= \bar{\mathcal{L}}_{2,+} - \bar{\mathcal{L}}_{3,+} = 2 \operatorname{Re}[(\bar{v}\bar{V} - \bar{a}\bar{A})^*(\bar{a}\bar{V} - \bar{v}\bar{A})].
\end{aligned} \tag{C2}$$

The result for the general cross section is simply

$$\frac{8s}{\alpha^2} \frac{d\sigma}{d\Omega} = (1 - \mathcal{O}_+^L \mathcal{O}_+^L) 4\mathfrak{B}_1 + (1 + \mathcal{O}_+^L \mathcal{O}_+^L) [(1 - \cos\theta)^2 \mathfrak{B}_2 + (1 + \cos\theta)^2 \mathfrak{B}_3] + \mathcal{O}_+^T \mathcal{O}_+^T \sin^2\theta [\cos 2\varphi \mathfrak{B}_4 + \sin 2\varphi \mathfrak{B}_5] \\ + (\mathcal{O}_+^L + \mathcal{O}_+^L) [(1 + \cos\theta)^2 \mathfrak{B}_6 + (1 - \cos\theta)^2 \mathfrak{B}_7] + (\mathcal{O}_+^L - \mathcal{O}_+^L) 4\mathfrak{B}_8. \quad (\text{C3})$$

In the case of  $e^-e^+ \rightarrow e^-e^+$  with the storage ring tuned to one resonance without overlapping another, the results for  $\mathfrak{B}_j$  analogous to Eq. (A15) are

$$\mathfrak{B}_1 = [s/t + (g_V^2 - g_A^2)Q]^2, \\ \mathfrak{B}_2 = [1 + 4\rho g_V R + 2\rho^2(3g_V^2 - g_A^2)R^2]\mathcal{D} \\ + 2[1 + (2\rho g_V + g_V^2 - g_A^2)R + \rho(\rho + 2g_V)(g_V^2 - g_A^2)R^2]\mathfrak{D} + [1 + (g_V^2 - g_A^2)R]^2, \\ \mathfrak{B}_3 = [1 + 4\rho g_V R + 6\rho^2(g_V^2 + g_A^2)R^2]\mathcal{D} \\ + 2\left\{1 + \frac{s}{t} + \left[\left(1 + \frac{s}{t}\right)2\rho g_V + g_V^2 + g_A^2\right]R + (g_V^2 + g_A^2)Q + \left(1 + \frac{s}{t}\right)\rho^2(g_V^2 + g_A^2)R^2 + 2\rho g_V(g_V^2 + 3g_A^2)R(R+Q)\right\}\mathfrak{D} \\ + \left(1 + \frac{s}{t}\right)^2 + 2\left(1 + \frac{s}{t}\right)(g_V^2 + g_A^2)(R+Q) + (g_V^4 + 6g_V^2g_A^2 + g_A^4)(R+Q)^2, \\ \mathfrak{B}_4 = 2[1 + 4\rho g_V R + 6\rho^2g_V^2R^2]\mathcal{D} \\ + 2\left\{1 + \frac{s}{t} + \left[\left(1 + \frac{s}{t}\right)2\rho g_V + g_V^2 + g_A^2\right]R + (g_V^2 + g_A^2)Q + \left(1 + \frac{s}{t}\right)\rho^2(g_V^2 - g_A^2)R^2 + 2\rho g_V(g_V^2 + g_A^2)R(R+Q)\right\}\mathfrak{D} \\ + 2\left[1 + \frac{s}{t} + \left(1 + \frac{s}{t}\right)(g_V^2 - g_A^2)R + (g_V^2 + g_A^2)(R+Q) + (g_V^4 - g_A^4)R(R+Q)\right], \\ \mathfrak{B}_5 = 4[\rho g_A R - g_V g_A(R-Q) + \rho(2\rho g_V + g_V^2 - g_A^2)g_A R^2 - 2\rho g_V^2 g_A R(R-Q)]\mathcal{G}, \\ \mathfrak{B}_6 = 4[\rho g_A R + 3\rho^2 g_V g_A R^2]\mathcal{D} \\ + 4\left[\left(1 + \frac{s}{t}\right)\rho g_A R + g_V g_A(R+Q) + \left(1 + \frac{s}{t}\right)\rho^2 g_V g_A R^2 + \rho(3g_V^2 + g_A^2)g_A R(R+Q)\right]\mathfrak{D} \\ + 4\left[\left(1 + \frac{s}{t}\right)g_V g_A(R+Q) + g_V g_A(g_V^2 + g_A^2)(R+Q)^2\right], \\ \mathfrak{B}_7 = \mathfrak{B}_8 = 0, \quad (\text{C4})$$

where

$$Q = (s/t)\bar{R} = s/e^2(t - M_W^2) \quad (\text{C5})$$

is approximately  $R$  at moderate  $s$ .

Radiation and spreading of the beam energies have the effect on the resonance of replacing  $\mathcal{D}$  with  $\mathcal{E}_e^0$  as in Eq. (1.2), and averaging the  $\mathfrak{D}$  terms to zero. The observed enhancement  $\mathcal{E}_e$  of  $d\sigma/d\cos\theta$  can be defined similar to Eq. (A17) using

$$\frac{d\sigma}{dz} = (\mathcal{E}_e + 1) \frac{d\sigma_b}{d\Omega}, \quad (\text{C6})$$

where

$$\frac{d\sigma_b}{dz} = \frac{\pi\alpha^2}{2s} \frac{(3+z)^2}{(1-z)^2} (1 + \delta_b) + \text{large QED corrections}, \\ \mathcal{E}_e = \mathcal{E}_e^0 \frac{(1+z^2)(1-z)^2}{(3+z^2)^2} \frac{(1 + \delta_r)}{(1 + \delta_b)} + \text{large QED corrections}.$$

The cross section for neutral lepton production  $e^-e^+ \rightarrow E^0\bar{E}^0$  with  $M_{E^0}$  neglected is given by Eq. (C3) if only the  $R$  terms in Eq. (A8) and their  $t$ -channel analogs,  $\bar{R}$  are used. In this case  $\bar{R}$ ,  $\bar{g}_{V,A}$ , and  $\bar{G}_{V,A}$  refer to the charged  $W^\pm$ , whereas  $R$ ,  $g_{V,A}$ , and  $G_{V,A}$  refer to the  $W^0$  as before. The latter will be enhanced by 1<sup>-</sup> resonances.

- \*Present address: Princeton University, Plasma Physics Laboratory, Princeton, New Jersey 08544.
- <sup>1</sup>R. Budny, Phys. Rev. D 14, 2969 (1976); Phys. Lett. 55B, 227 (1975); 58B, 338 (1975).
- <sup>2</sup>E. Fischbach, B. Kayser, and S. P. Rosen, Phys. Rev. D 11, 2547 (1975); G. Pócsik, Ann. Phys. (N.Y.) 105, 259 (1977).
- <sup>3</sup>R. Budny and A. McDonald, Phys. Rev. D 10, 3107 (1974).
- <sup>4</sup>R. Budny and A. McDonald, Phys. Rev. D 16, 3150 (1977).
- <sup>5</sup>S. W. Herb *et al.*, Phys. Rev. Lett. 39, 252 (1977); W.R. Innes *et al.*, *ibid.* 39, 1240 (1977).
- <sup>6</sup>Ch. Berger *et al.*, Phys. Lett. 76B, 243 (1978); C. W. Darden *et al.*, *ibid.* 76B, 246 (1978); 78B, 364 (1978).
- <sup>7</sup>C. W. Darden *et al.*, Phys. Lett. 80B, 419 (1979).
- <sup>8</sup>D. Yennie, Phys. Rev. Lett. 34, 239 (1975).
- <sup>9</sup>F. A. Berends, K. J. F. Gaemers, and R. Gastmans, Nucl. Phys. B57, 381 (1973); B63, 381 (1973).
- <sup>10</sup>B. Ya. Zel'dovich and M. V. Terent'ev, Yad. Fiz. 7, 1083 (1968) [Sov. J. Nucl. Phys. 7, 650 (1968)].
- <sup>11</sup>F. A. Berends, K. J. F. Gaemers, and R. Gastmans, Nucl. Phys. B68, 541 (1974).
- <sup>12</sup>Y.-S. Tsai, Phys. Rev. D 4, 2821 (1971); 13, 771 (E) (1976).
- <sup>13</sup>T. Kinoshita and A. Sirlin, Phys. Rev. 108, 844 (1957). The values of  $\delta$  and  $\xi$  have been scaled by a factor of 3 so that  $\rho$ ,  $\delta$ , and  $\xi$  are  $\frac{3}{4}$ ,  $\frac{3}{4}$ , and  $\frac{1}{3}$  for V-A decay, and 0, 0, and 1 for V+A.
- <sup>14</sup>R. Budny and A. McDonald, Phys. Rev. D 15, 81 (1977).